and the area is given by the determinant

$$2A^{(e)} = \begin{vmatrix} 1 & 1 & 1 \\ x_i & x_j & x_k \\ y_i & y_j & y_k \end{vmatrix} \tag{A.22}$$

Similar expressions may be found in [9].

The same analysis can be carried out for a rotating bearing such as a journal, partial arc, or multilobed bearing. Consider a shaft of radius R rotating with angular velocity ω_j in a journal bearing rotating with angular velocity ω_b. To maintain consistency in coordinate systems, unwrap the bearing and journal as in Fig. 5. Now, as before, the z-direction is across the film while an x and y may be used to locate the nodes. Equations (A.16), (A.19), and (A.20) remain the same while Equations (A.17) and (A.18) become

$$K^{(e)}_{fxn} = \left[\frac{\rho h}{4} R(\omega_b + \omega_j) b_n\right]^{(e)} \tag{A.23}$$

$$K^{(e)}_{fyn} = 0 \tag{A.24}$$

Note that $x = R\theta$ in equations (A.21) and (A.22).

DISCUSSION

S. M. Rohde[2]

The authors have presented some interesting numerical results pertaining to the application of finite element methods to lubrication problems. Their conclusions regarding mesh orientation and refinement agree with our own experience. In fact, in [20][3] an analysis of the linear equation at each node arising in both the finite difference and finite element formulations for the squeeze film problem was performed. Numerical comparisons similar to those presented in this paper were presented there. In particular, it was shown that the pressure distribution corresponding to (in the present paper) FEM #2 is everywhere greater than that of FEM #3.

A key and perhaps the most important point which the authors make is that for rectangular or "rectangular-like" regions the FEM topology becomes particularly simple leading to reduced bandwidth, etc. Furthermore, a large class of lubrication problems fall into this category. These facts were noted several years ago by the discussor [21]. Likewise it was also noted in [2] that such an "indexing" could be efficiently used to incorporate Reynold's boundary condition with an iterative scheme. More recently that construction was proven [22].

As noted in [21], any region which is "mappable" into a unit square can be indexed like the unit square. In this respect the unit square is a "canonical" region. Recent advances in automatic mesh generation [23, 24] have been based on precisely such mappings. We have recently used this approach (and some modifications) for generating two and three dimensional finite element discretizations. We will now illustrate the potential of the method of generating a FEM mesh via some examples. The reader is referred to [23, 24] for a complete treatment.

Basically, as shown in Fig. 7, a mapping is desired which maps the unit square S, $0 \le s \le 1$, $0 \le t \le 1$ onto the region R which is to be discretized. The mapping [25] is to take the interior of S onto the interior of R and the boundaries of S onto the boundaries of R. Every point in the interior of R is to be the image of a unique point in S. Denoting the four boundaries (curves) of R by $\mathbf{f}_i$ as shown, in Fig. 7 a bilinearly blended transfinite interpolant may be written as

$$\begin{Bmatrix} x(s,t) \\ y(s,t) \end{Bmatrix} = \mathbf{F}(s,t) = (1-s)\mathbf{f}_1(t) + s\mathbf{f}_2(t) + (1-t)\mathbf{f}_3(s) + t\mathbf{f}_4(s) - (1-s)t\mathbf{f}_1(1) - s(1-t)\mathbf{f}_2(0) - (1-s)(1-t)\mathbf{f}_3(0) - st\mathbf{f}_4(1)$$

Equation (1) provides a suitable mapping of the interior (and boundaries) of S onto the interior (and boundaries) of R. Our experience with equation (1), which represents the simplest form of the transfinite interpolant [23, 24], has been very good. To use this representation one merely programs the four parameterizations of the

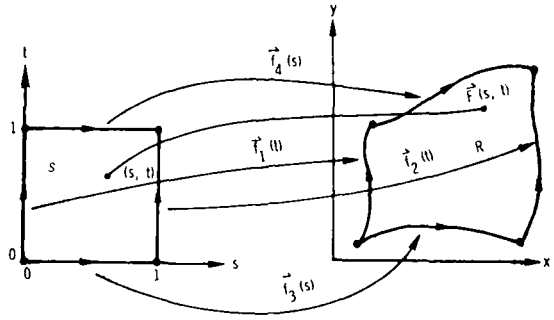

Fig. 7

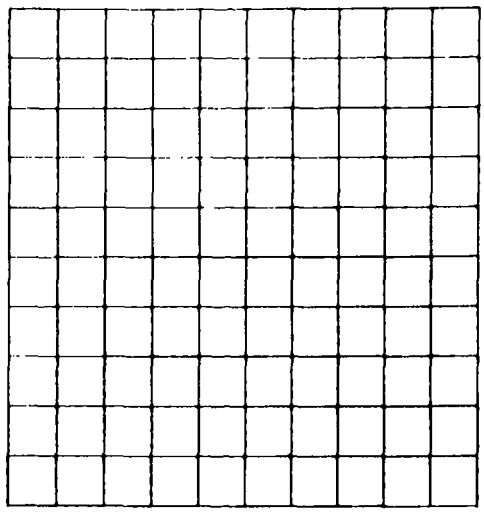
Fig. 8(a)

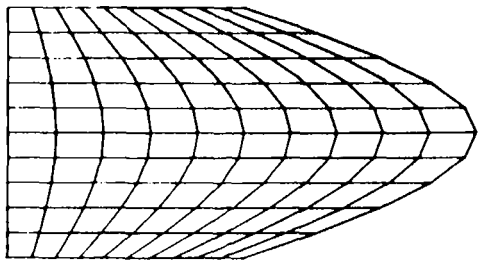
Fig. 8(b)

[2] Research Laboratories, General Motors Corp., Warren, Mich.

[3] Numbers in brackets designate Additional References at end of paper.

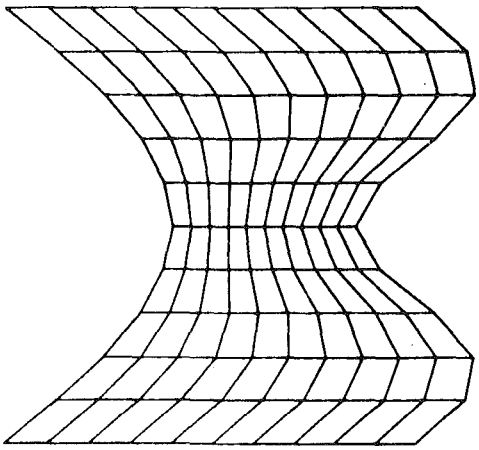

Fig. 8(*c*)

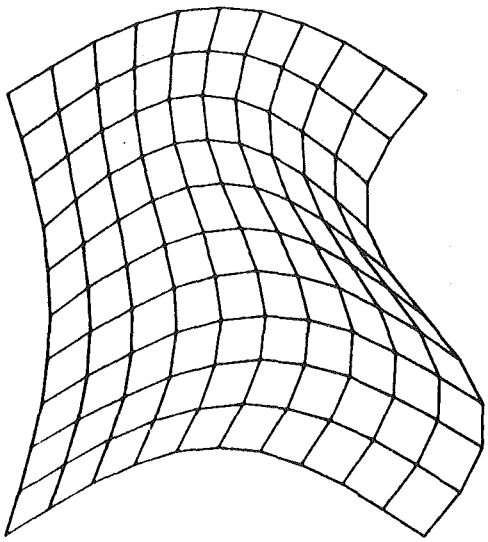

Fig. 8(*d*)

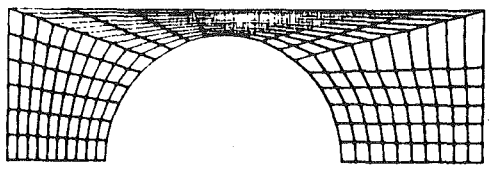

Fig. 8(*e*)

boundaries. Picking these parameterizations as well as the appropriate four boundaries can, however, sometimes require some experimentation. Here an interactive graphics terminal is almost mandatory. Figure 2a shows a uniform 10 × 10 mesh dividing S. Fig. 8(b) shows a simple mapping in which

$$\mathbf{f}_1(t) = \begin{Bmatrix} 0 \\ t \end{Bmatrix}$$

$$\mathbf{f}_2(t) = \begin{Bmatrix} 1 + \sin \pi t \\ t \end{Bmatrix}$$

$$\mathbf{f}_3(s) = \begin{Bmatrix} s \\ 0 \end{Bmatrix}$$

$$\mathbf{f}_4(s) = \begin{Bmatrix} s \\ 1 \end{Bmatrix}.$$

Fig. 8(c) shows a more severe situation in which

$$\mathbf{f}_1(t) = \begin{Bmatrix} 0.4 \sin \pi t \\ t \end{Bmatrix}$$

$$\mathbf{f}_2(t) = \begin{Bmatrix} 1 + 0.2 \sin 3\pi t \\ t \end{Bmatrix}$$

$$\mathbf{f}_3(s) = \begin{Bmatrix} s \\ 0 \end{Bmatrix}$$

$$\mathbf{f}_4(s) = \begin{Bmatrix} s \\ 1 \end{Bmatrix}.$$

In Fig. 8(d) we have

$$\mathbf{f}_1(t) = \begin{Bmatrix} 0.1 \sin \pi t \\ t \end{Bmatrix}$$

$$\mathbf{f}_2(t) \begin{Bmatrix} 1 + 0.15 \sin 2\pi t \\ t \end{Bmatrix}$$

$$\mathbf{f}_3(s) = \begin{Bmatrix} s \\ 0.2 \sin \pi s \end{Bmatrix}$$

$$\mathbf{f}_4(s) = \begin{Bmatrix} s \\ 1 + 0.2 \sin \pi s \end{Bmatrix}.$$

Finally in Fig. 8(e) we have

$$\mathbf{f}_1(t) = \begin{Bmatrix} 0.2(1 - t) \\ 0 \end{Bmatrix}$$

$$\mathbf{f}_2(t) = \begin{Bmatrix} 1 - 0.3((1 - t) \\ 0 \end{Bmatrix}$$

$$\mathbf{f}_3(s) = \begin{Bmatrix} 0.45 - 0.25 \cos \pi s \\ 0.25 \sin \pi s \end{Bmatrix}$$

$$\begin{Bmatrix} 0 \\ s \end{Bmatrix}, 0 \le S \le 0.3$$

$$\mathbf{f}_4(s) = \begin{Bmatrix} (s - 0.3)/0.4 \\ 0.3 \end{Bmatrix}, 0.3 < s \le 0.4$$

$$\begin{Bmatrix} 1.0 \\ (1.0 - s) \end{Bmatrix}, 0.7 < s \le 1$$

In conclusion it should be emphasized that the inclusion of an automatic mesh generation scheme such as presented in this discussion represents an extremely simple addition to a finite element lubrication code and is well worth the effort.

Additional References

20 Rohde, S. M., Discussion of "Application of Finite Element Methods to Lubrication: Squeeze Films between Porous Surface," by Eidelberg, B. E. and Booker, J. F., JOURNAL OF LUBRICATION TECHNOLOGY TRANS, ASME, Series F, Vol. 98, No. 1, Jan. 1976.

21 Rohde, S. M., "Finite Element Optimization of Finite Stepped Slider Bearing Profiles," *TRANS ASLE*, Vol. 17, 2, 1974.

22 Rohde, S. M. and McAllister, G. T., "A Variational Formulation for a Class of Free Boundary Problems Arising in Hydrodynamic Lubrication," *Int. J. Engrg. Sci.*, Vol. 13, 1975.

23 Gordon, William J., and Hall, Charles A., "Geometric Aspects of the Finite Element Method," in *The Mathematical Foundations of the Finite Element Method with Applications to Partial Differential Equations*, edited by A. K. Aziz, Academic Pres, New York, 1972.

24 Gordon, William J., and Hall, Charles A., "Construction of Curvilinear Co-ordinate Systems and Application to Mesh Generation," *Int. J. Num. Methods in Engineering*, Vol. 7, 1973, pp. 461–477.

J. F. Booker[4]

It is a good sign to find so many authors and discussors using the finite element method in lubrication. The method has come a long

[4] Associate Professor, School of Mechanical and Aerospace Engineering, Cornell University, Ithaca, N. Y.

way in quite a short time (as these things are measured).

The present paper and much of the earlier discussion centers on the mapping of bearing pads onto a generic rectangle for purposes of mesh generation. While this is certainly appropriate for many bearing and grooving geometries, the resulting regularity of nodal spacing is of some concern. One of the great putative advantages of the finite element method over the competing finite difference method is the ease with which meshes can be refined *locally* as required for solution accuracy. One hopes that this possibility is not being compromised too greatly in the schemes of the authors and discussors.

The authors have considered in some detail the matter of optimal mesh design. The finding that meshes should be finest in regions of high pressure gradients is, of course, not unexpected. It leads immediately to the awkward situation (found in other application fields as well) that the optimum *problem* formulation depends on the *solution*! The iterative process suggested by this paradox is being pursued actively in the structural mechanics field at present; perhaps some impact of that work will be felt in our own field before too long.

A. Curnier[5]

Along the plan followed by the authors, three subjects may be distinguished:

1 The pressure variational principle formulation which is quite classical and does not call for any comment;

2 the bandwidth minimization: the current trend is to relieve the user from being too much concerned with minimizing the bandwidth of his mesh by using, for instance, profile storage and solvers;

3 the mesh design optimizations: the paper provides very helpful practical guidelines for the user to design a near optimal mesh based on the intuitive picture of the solution:

(*a*) Align the diagonals dividing the preliminary quadrilaterals into the definitive triangular elements with the expected pressure gradient directions

(*b*) concentrate nodes where large pressure gradients are expected.

These two qualitative results can be explained and to some extent quantified as it is sketched now:

(*a*) Linear elements do preserve the continuity of pressure gradients inside an element and hereby along each side of the diagonal element interfaces: they do not preserve it across such diagonals. Result 3 (a) is a consequence of this remark..

(*b*) For a linear element used to solve a second order elliptic problem like the one at hand, the error pressure is expected to decrease as the square of the mesh refinement:

if p = exact pressure
p^h = f.e.m. pressure
h = mesh coarseness characteristic dimension (h = max $|h_j|$, h_j = side length of triangle j = 1,3
C = constant (element, p^h)
$||p||_s^2 = \int_\Omega (p^2 + p'^2 + \ldots + p^{(s)2}) d\Omega$
then $||p - p_h||_s = C_s h^{2-s}$ and in particular
$||p - p_h||_0 = C_0 h^2$

Therefore the only limitation on the rate of convergence (for a given problem and a given element) is the smoothness of the solution p.

The above rate of convergence is in the mean, for a regular mesh and without singularities. The pointwise convergence rate can be expected to be the same for a smooth solution and in fact

$$|p_e - p_{he}|_s \leq C_s h^{2-s} |p_e|_2$$

where e = element

$$|p|_s^2 = \int_\Omega (p^{(s)2}) d\Omega$$

Since h, μ, u_x, u_y are chosen constant over an element, the solution p exhibits singularities (probably more drastic as h decreases). With a regular mesh, the order of convergence will definitely be reduced. However, by properly grading the mesh (that is by keeping $h_e^{2-s} |p_e|_2$ roughly the same from one element to the next) the same order of accuracy can be achieved for a triangular as for a regular solution p.

Finally, it is recalled that the strict Ritz procedure always corresponds to an approximation which is too "stiff." The discrete energy exceeds the exact one which corresponds to an underestimate of the pressure gradients and pressures. This is true in the mean only since the link between energy and pressure is not strictly monotone. In other words p^h may exceed p in some parts of the mesh and still have smaller derivatives in the mean square sense. This can be changed by using a dual or hybrid formulation.

Results concerning rectangular and higher order elements can be obtained along the same lines.

[5] Ph.D. student, Division of Structural Engineering and Structural Mechanics, University of California, Berkeley, Calif.

Authors' Closure

The authors would like to thank the three discussers of the paper for their constructive comments. We are glad to see so much interest in the method developed here as we feel it provides detailed structure to material noted by other authors where little is explored in depth.

In the first discussion, substantial agreement with the authors work for the squeeze film problem is noted and some additional recent references are included. A useful mesh generation scheme particularly suited to the matrix labeling technique employed in the paper is presented. It appears to the authors that the matrix labeling facilitates automatic mesh generation of this and other types. In fact, the development of practical analysis computer programs for nonresearch engineers almost requires automatic schemes.

The second discusser is to be strongly commended for his excellent work in finite element analysis. It seems that the question of refining meshes locally has usually been done by adding a few extra nodes in the region where greatest accuracy is desired. Often in complex structural problems many of the nodes are assigned by hand so that adding another few nodes is much easier than regenerating a substantial portion of the mesh. Perhaps it is time to consider that the flexibility of the finite element method should be used to concentrate the grid points in the desired region using a combination of automatic mesh generation scheme and some sort of simple user assigned concentration factor. Simply adding a few nodes in one region can greatly increase the matrix bandwidth (and solution time) for the sake of only a few additional nodes. It should be emphasized again that the method developed in the paper does not depend in any way upon the regularity of nodal spacing but only on the regularity of the nodal numbering process. The relation between the two depends upon the ingenuity of the programmer.

In the third discussion the comments are more mathematical in nature. The continuity of pressure gradients preserved along the sides of elements, but not across them, has been observed by Oden [10] and other authors. Noting this point does, however, contribute to understanding the results for optimum alignment of the diagonals. Certainly much more work can be done with regard to other element configurations.

In the time since the paper was written and accepted for publication, the method described here has been applied to many practical applications. It has proved useful in analysing partial arc, axial groove, multilobe, tilting pad, and pressure dam bearings. In most industrial applications the load is known while the equilibrium position must be found by an iterative process. A coarse grid system using approximately 3 axial node points and 9 circumferential node points per pad is used to obtain a first estimate of the equilibrium eccentricity

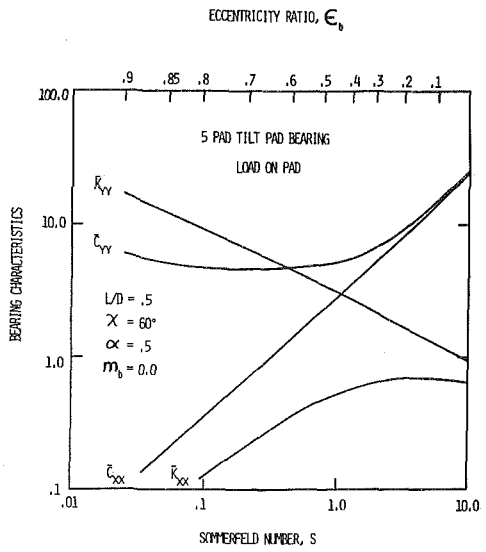

Fig. 9 Bearing characteristics versus Sommerfeld number and eccentricity ratio for a 5 pad tilt pad bearing

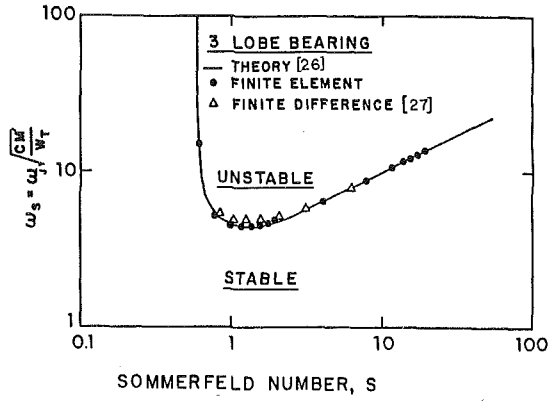

Fig. 10 Stability threshold versus Sommerfeld number for three pad multilobe bearing. 100° pad arc length, offset factor 0.8, preload 0.7, load on center of pad, *L/D* = 0.75

and attitude angle. Then a full grid system of, say, 5 by 31 nodes per pad is employed. For eccentricities around 0.5, this reduces the number of full grid iterations to 2 or 3. A casual survey of computer execution times indicates approximately a 50 percent saving by using the coarse grid system. Numerical differentiation is then used to determine dynamic coefficients and the Routh criteria used for the stability of each bearing. Thus even the linearized bearing analysis, as opposed to a transient one, for a four pad multilobe bearing can involve 36 solutions of Reynolds equation to obtain the equilibrium position. This includes taking four pads per evaluation, three evaluations to determine the appropriate slopes for a Newton Raphson iterative process, and three iterations. Furthermore, 32 more evaluations are required to determine the dynamic coefficients (taking four pads and central differences for the coefficients). The situation is much worse for tilt pad bearings when pad iterations are necessary. Clearly the consideration of error and computer time saving is not merely academic.

To further demonstrate the practical applicability of the method outlined in this paper, Fig. 9 presents stiffness and damping coefficients for a 5 pad tilt pad bearing. These coefficients were determined using the finite element analysis outlined here and the pad assembly method [25].[6] These coefficients may be used in critical speed and stability programs when rotor-bearing systems are analyzed. Also, these coefficients may be employed in a linear time transient program. Finally, the characteristics may be used in a simple stability analysis for the bearing. A sample stability curve is shown in Fig. 10 for a 3 pad multilobe bearing where

$$L/D = .75$$

$$\chi = 100°$$

$$\alpha = .8$$

$$m_b = .7$$

and the loading is on the center of the bottom pad. The finite element solution is compared to a long bearing solution with end leakage correction [26] and a finite difference solution [27]. The stability parameter, ω_s, is discussed in detail in references [26] and [28].

Additional Nomenclature

c = pad radial clearance, (mm)

c_b = bearing radial clearance, (mm)

C_{xx}, C_{yy} = principal horizontal, vertical damping coefficients, (N-s/mm)

$\bar{C}_{xx}$, $\bar{C}_{yy} = C_{xx}\frac{c\omega_j}{W_T}$, $C_{yy}\frac{c\omega_j}{W_T}$, dimensionless principal horizontal, vertical damping coefficients

D = bearing diameter, (mm)

K_{xx}, K_{yy} = principal horizontal, vertical stiffness coefficients, (N/mm)

$\bar{K}_{xx}$, $\bar{K}_{yy} = K_{xx}\frac{c}{W_T}$, $K_{yy}\frac{c}{W_T}$, dimensionless principal horizontal, vertical stiffness coefficients

L = bearing length (mm)

M' = journal mass (N-s^2/mm)

$m_b = 1 - \frac{c_b}{c}$, bearing preload factor

N_s = journal rotational speed, (rev/s)

$S = \frac{\mu N_s LD}{W_T}\left(\frac{R}{c}\right)^2$, Sommerfeld number

W_T = bearing external load, (N)

$\alpha = \frac{\theta_p}{\chi}$, bearing offset factor

ϵ_b = bearing eccentricity ratio

θ_p = angle from leading edge of pad to pad pivot point, (degrees)

χ = pad arc length, (degrees)

$\omega_s = \omega_j\sqrt{\frac{cM'}{W_T}}$, stability parameter

Additional References

25 Lund, J. W., "Spring and Damping Coefficients for the Tilting-Pad Journal Bearing," *Trans. ASLE*, Vol. 7, No. 4, Oct. 1964, pp. 342–352.

26 Eierman, R. M., "Stability Analysis and Transient Motion of Axial Groove, Multilobe, and Tilting Pad Bearings," MS thesis, University of Virginia, Aug. 1976.

27 Lund, J. W., "Rotor-Bearing Dynamics Design Technology, Part VII: The Three Lobe Bearing and Floating Ring Bearing," Mechanical Technology Incorporated, Technical Report No. AFAPL-TR-65-45, Feb. 1968.

28 Barrett, L. E., Gunter, E. J., and Allaire, P. E., "Stability and Dynamic Response of Pressurized Journal Bearings with Nuclear Water Pump Applications," to be published in *Annals of Nuclear Energy*.

[6] Numbers 25–28 in brackets designate Additional References at end of closure.